Competition between Different Symmetries in Convective Patterns

S. Ciliberto,[(1)] E. Pampaloni,[(1)] and C. Pérez-García[(2)]

[(1)]*Istituto Nazionale di Ottica, Largo Enrico Fermi 6, 50125 Arcetri-Firenze, Italy*

[(2)]*Departament de Física, Universitat Autonoma de Barcelona, 08193 Bellaterra, Barcelona, Catalonia, Spain*

(Received 11 May 1988)

The transition between hexagons and rolls in convective patterns has been studied in pure water under non-Boussinesq conditions. The transition is characterized qualitatively by shadowgraph images and quantitatively by heat-flow measurements and a local technique based on the deflections of a laser beam. We also show that with this local technique one can recover global quantities such as the convective heat flow.

PACS numbers: 47.20.Bp, 47.25.Qv

Patterns with different symmetries can develop in Rayleigh-Bénard convection.[1] Under normal conditions a pattern of rolls arises above the critical threshold. When the convective cell has an insulating upper plate,[2,3] or in binary mixtures in the Soret-driven regime,[4] a pattern of squares is the preferred structure. Hexagonal cells can appear when the transport coefficients of the fluid are temperature dependent (non-Boussinesq conditions)[5,6] or when an external modulation of temperature is applied.[7]

The purpose of the present Letter is to show experimental results on the transition between hexagons and rolls under non-Boussinesq conditions. Some experimental[5] and theoretical[6] analyses demonstrate the existence of such a transition. These analyses deal often with global characteristics of the pattern. We present in this paper a quantitative analysis of the dynamics of pattern competition, from global and local measurements.

The experiment was performed in a cylindrical convective cell of diameter $D=72$ mm and depth $d=2.00$ mm (aspect ratio $\Gamma=D/2d=18$). The lateral wall is made of Plexiglas. The inner wall is not vertical, but it has a triangular ramp in order to reduce the horizontal thermal gradients.[7c] The bottom and the top plates are made of copper and sapphire, respectively. The upper plate, which allows for optical inspection, is cooled on its top by a circulation of temperature-stabilized water. The copper plate has the upper surface polished to a mirror finish and covered with nickel and gold films. An electric resistor heats this plate. The cell is contained in a temperature-stabilized box. This ensures a temperature stability about ± 0.001 K. The working fluid is pure water at mean temperature of 28 °C whose Prandtl number is $P=5.81$. The horizontal diffusion time is $\tau_h=D^2/4\kappa=2.45$ h.

The general features of the pattern are determined qualitatively by a shadowgraph technique. Heat-flow and optical measurements enable us to obtain quantitatively global and local characteristics of the patterns. The optical technique is based on the deflections of a laser beam that crosses the fluid layer. Details of this method have been described elsewhere[8] and applied to measure convective motions.[9] The actual setup allows us to obtain, with a twelve-bit resolution, the two components of the horizontal thermal gradient $(\partial T/\partial x, \partial T/\partial y)$ measured on an array of 128×128 points on a square area of 4.9×4.9 cm^2. This allows us to reconstruct the temperature field $T(x,y)$ averaged on the vertical direction. The accuracy of the measurement is about 7%, the sensitivity 10^{-2} K/mm, and the spatial resolution about 0.5 mm.

With the aspect ratio ($\Gamma=18$) of our cell, the corresponding critical Rayleigh number is $R_c=1714$.[10] Taking the value of the transport coefficients at the mean temperature of the cell, one obtains the critical temperature difference $\Delta T_c^t=12.58$ K.[11] This temperature difference is sufficient to induce variations in the thermal expansion coefficient and in the viscosity (non-Boussinesq effect). However, in the present experiment these effects are small and can be considered as a perturbation in the nonlinear regime, as assumed in theoretical calculations made by Busse.[6c]

Inserting the values of the non-Boussinesq corrections ($P=2.0$) in the equations of Ref. 6c, we obtain the following thresholds for the stability of hexagons and rolls: $\epsilon_A=-5.5\times10^{-4}$, $\epsilon_R=5.3\times10^{-2}$, and $\epsilon_H=0.18$, where ϵ_A is the minimum value of $\epsilon=(\Delta T-\Delta T_c)/\Delta T_c$ for hexagonal motions, ϵ_R the minimum ϵ for which the rolls are stable, and ϵ_H the maximum ϵ for which hexagons are stable.

The value of ϵ_A indicates that a region of *subcritical* instability cannot be observed with the resolution of the present experiment. The last two values limit the interval in which hexagonal cells can be stable. Above ϵ_H only rolls are stable. Between these two values, however, hysteresis between hexagons and rolls can appear.

The critical temperature, obtained from heat-flow measurements, turns out to be $\Delta T_c=12.60\pm0.02$ K, in good agreement with the theoretical one.[12] (In the following, this value will be used in the definition of ϵ.) Figures 1(a) and 1(b) show the shadowgraph images of two typical patterns obtained at $\epsilon=0.02$ and 0.14, re-

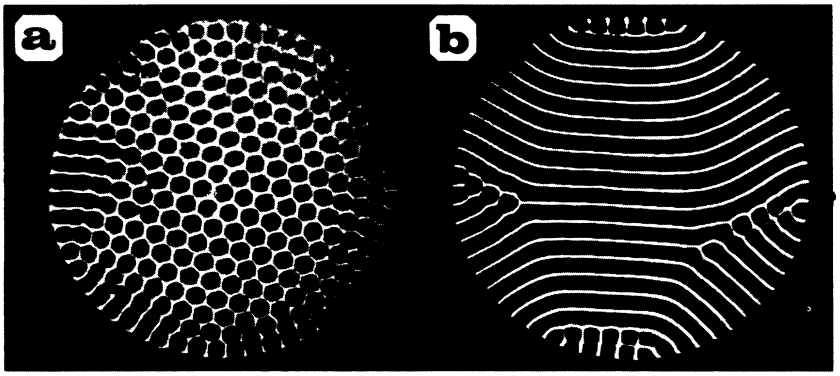

FIG. 1. Shadowgraph images of convective patterns. (a) Hexagonal pattern for $\epsilon=0.02$. (b) Pattern of rolls for $\epsilon=0.14$.

spectively. A transition between a hexagonal pattern and a pattern of rolls is clearly seen. Very near threshold the pattern consists of a regular array of hexagons surrounded with some zones in which rolls seem to destabilize the pattern. These correspond to zones where the lateral boundary conditions are not compatible with the hexagonal symmetry. It is remarkable to observe that inside the hexagonal pattern there are no defects. This pattern is reproducible and stationary for more than $5\tau_h$. Figure 1(b) shows how one set of rolls finally survives. Indeed, the pattern is mainly formed by rolls with a very regular orientation in the center of the cell, and with two opposite areas of defect combinations that form grain boundaries. Two dislocation zones where hexagons prevail can also be observed. This final pattern is very similar to that obtained by some authors[13] in convection under normal (Boussinesq) conditions. However, the pattern remains stationary for more than $54\tau_h$ in our case.

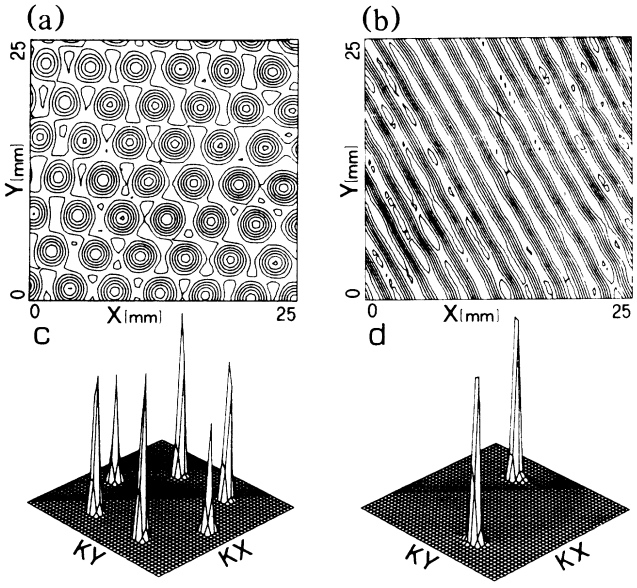

FIG. 2. Temperature-field reconstruction from the horizontal gradient. (a) Hexagonal pattern for $\epsilon=0.02$. The temperature difference between two isotherms is 0.21 K. (b) Rolls for $\epsilon=0.14$. The isotherms are separated by 0.42 K in this case. Fourier spectra of the temperature field in the full scanning area for the same values of ϵ as in (a) and (b): (c) for hexagons; (d) for rolls.

The deflection technique gives more detailed information about the convective fields. For a fixed ϵ and after a time sufficient to stabilize the pattern, a scan is made on the system. The horizontal temperature gradient is measured for 27 rising values of ϵ in the interval $0.00 \leq \epsilon \leq 0.14$. When the maximum of ϵ is attained, the measurements are repeated by decreasing ϵ. The horizontal temperature field $T(\mathbf{r})$ is obtained by integration of the gradient $(\partial T/\partial x, \partial T/\partial y)$. Figures 2(a) and 2(b) show two examples of the reconstruction of $T(\mathbf{r})$ in the central part of the scanning area for $\epsilon=0.02$ and 0.14, respectively. Figures 2(c) and 2(d) illustrate the Fourier spectrum of $T(\mathbf{r})$ calculated in the full scanning area. The peaks in Figs. 2(c) and 2(d) are very sharp and their amplitudes are comparable. This confirms that almost perfect patterns develop.

The nondimensional convective heat flow $\mathcal{N}$ is defined as

$$\mathcal{N}=(N-1)R/R_c=\sum_{\mathbf{k}}|\Psi_{\mathbf{k}}|^2, \tag{1}$$

where N here denotes the Nusselt number. The $\Psi_{\mathbf{k}}$ are the nondimensional amplitudes of the Fourier modes of the temperature field; that is

$$T(\mathbf{r})=(\Delta T_c\langle\theta_0\rangle/\alpha R_c)\sum_{\mathbf{k}}\Psi_{\mathbf{k}}\exp(i\mathbf{k}\cdot\mathbf{r}). \tag{2}$$

Here $\langle\theta_0\rangle$ stands for the nondimensional temperature perturbation averaged on the vertical direction and α is a normalization factor, introduced to satisfy Eq. (1). These two coefficients are obtained by the application of the normalization of Ref. 14 and the theoretical results of Ref. 15. After some calculations the dependence of $\mathcal{N}$ on ϵ is determined.

This dependence is shown in Fig. 3(a). Experimental points lie on two straight lines, one for hexagons in the interval $0.00 \leq \epsilon \leq 0.04$, and one for rolls for $0.04 \leq \epsilon \leq 0.14$. (The error in these experimental points

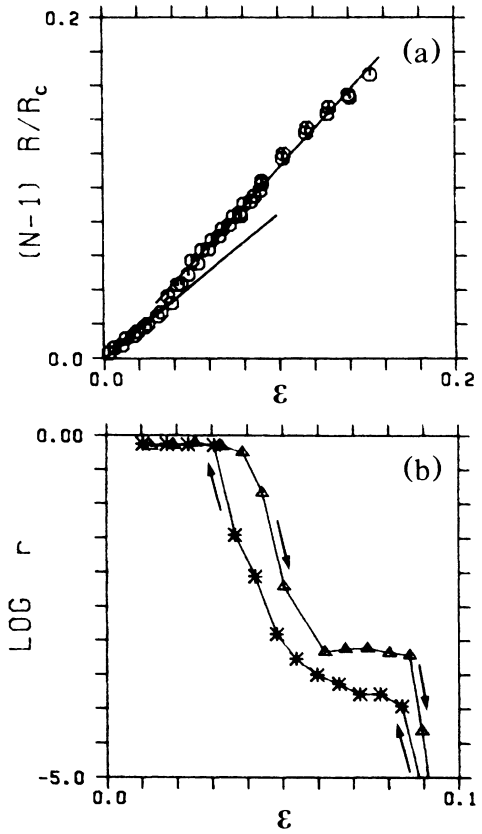

FIG. 3. (a) Nondimensional convective heat flow $\mathcal{N}$. (b) Normalized sum of the two modes ϕ_2 and ϕ_3 at $2\pi/3$ rad with respect to the surviving mode ϕ_1 ($r=[\phi_2+\phi_3]/2\phi_1$). The arrows indicate the different evolutions of the vanishing modes ϕ_2,ϕ_3 when ϵ increases or decreases.

is about $\pm 2\%$.) The slopes of these straight lines are obtained from a linear best fit of these results. They are $\gamma_H=0.86\pm0.03$ and $\gamma_R=1.13\pm0.02$. (This fit allows us also to verify the convective threshold obtained by heat-flow measurements with an error $\Delta\epsilon=1\times10^{-3}$.) These slopes are in perfect agreement, within the experimental errors, with those obtained with heat-flow measurements ($\gamma_H=0.89\pm0.02$, $\gamma_R=1.15\pm0.02$). The main source of error in Fig. 3(a) comes from the determination of the vertical scale. This accumulates the uncertainties of several conversion factors of the experimental system [sensitivity of the photodiodes, variations of the refractive index with temperature, finite area taken to make the fast Fourier transform of $T(\mathbf{r})$, etc.]. These uncertainties give an error of about 10% in the vertical scales in Fig. 3 and, consequently, in the slopes.

The slope values γ_H and γ_R in the present experiment, however, are in between those calculated theoretically from Ref. 16 for a laterally infinite system and $P=5.81$ ($\gamma_H=1.106$, $\gamma_R=1.431$) and those obtained by Walden and Ahlers[17] ($\gamma_H=0.69$, $\gamma_R=0.82$) for liquid helium ($P=0.78$) in a small cylindrical cell ($\Gamma=4.72$). Moreover, the ratio between those slopes, which must be independent of Γ and of the errors in the vertical scale, is $\gamma_R/\gamma_H=1.30\pm0.05$ in very good agreement with the theoretical value $\gamma_R/\gamma_H=1.294$ obtained from Ref. 16. To the best of our knowledge, this is the first time that a global parameter (convective heat flow) was obtained from a local measurement.

The square amplitudes, ϕ_i, of the three sets of rolls are obtained by means of the relation

$$\phi_i=\sum_{\mathbf{k}^*}|\Psi_{\mathbf{k}^*}|_i^2. \tag{3}$$

This sum is over pairs of conjugate peaks. It extends over wave numbers such as $k_{x,y}^{\max}-\beta\le k_{x,y}^{*}\le k_{x,y}^{\max}+\beta$, where $\mathbf{k}^{\max}$ is the wave vector corresponding to the maximum of the peak and β is twice the half-width of this peak. In order to characterize quantitatively the transition from hexagons to rolls, we have plotted in Fig. 3(b) the ratio $r=(\phi_2+\phi_3)/2\phi_1$ as a function of ϵ on a logarithmic-linear scale. Here ϕ_1 is the amplitude of the surviving mode and ϕ_2,ϕ_3 are the amplitudes of the two modes (at $2\pi/3$ rad with respect to the first one) which finally vanish. In Fig. 3(b) the high plateau ($r\simeq1$) corresponds to hexagons, while the transition to a pattern of rolls is characterized as the limit $r\to0$. From this figure one can deduce that a transition from hexagons to rolls (vanishing of two amplitudes) occurs between $\epsilon_R=(3.0\pm0.1)\times10^{-2}$ and $\epsilon_H=0.090\pm5\times10^{-3}$. It is smooth and hysteretic: smooth, because the pattern of hexagons is not suddenly replaced by a pattern of rolls; hysteretic, because the pattern is not the same by increasing or decreasing ϵ. These transition values are lower than $\epsilon_R^l=5.3\times10^{-2}$ and $\epsilon_H^l=0.18$ obtained from Ref. 6c for a laterally infinite system. However, the ratio ϵ_H/ϵ_R, which is independent of the strength of the non-Boussinesq effects,[6c] gives an experimental value of $\epsilon_H/\epsilon_R=3.0\pm0.27$, slightly smaller than $\epsilon_H^l/\epsilon_R^l=3.44$. Using equations (8.11) of Ref. 6c with the experimental values of γ_H, γ_R, and ϵ_H/ϵ_R instead of the corresponding theoretical ones yields consistency with the decreasing of the transition thresholds ϵ_R,ϵ_H. Shadowgraph and deflection techniques show that the rolls normal to the lateral walls tend to destabilize the hexagonal pattern, thus reducing the transition thresholds. The results in Ref. 17 and those in the present work indicate that the role played by the lateral walls and by defects on the non-Boussinesq convection is not yet well understood. Our observations suggest that this role cannot be fully characterized by global measurements (i.e., Nusselt number), but these must be supplemented by some local techniques. Moreover, a generalization of the theoretical results of Busse[6c] to account for the dynamics of defects on the transition becomes necessary for enlightenment on this problem.

We thank F. T. Arecchi, P. Bigazzi, P. Coullet, and P. Hohenberg for fruitful comments and L. Albavetti and M. D'Uva for very efficient technical assistance.

This work has been partially supported by the Gruppo Nazionale di Struttura de la Materia (Italy) and by the Comisión Asesora de Investigación Cientifica y Tecnica (Spain) of the Spanish Government. One of us (C.P.-G.) also acknowledges the support of the Fundación "Conde de Barcelona" (Barcelona, Spain).

[1]F. H. Busse, Rep. Prog. Phys. **41**, 1931 (1978).

[2]F. H. Busse and N. Rihai, J. Fluid Mech. **96**, 243 (1980); M. H. Proctor, J. Fluid Mech. **113**, 469 (1981).

[3]P. Le Gal, A. Pocheau, and V. Croquette, Phys. Rev. Lett. **54**, 2501 (1985).

[4]E. Moses and V. Steinberg, Phys. Rev. Lett. **57**, 2018 (1986).

[5]P. S. Sliveston, Forsch. Ing. Wes. **24**, 29, 59 (1959); C. Q. Hoard, C. R. Robertson, and A. Acrivos, Int. J. Heat Mass Transfer **13**, 849 (1970); M. Dubois, P. Bergé, and J. E. Wesfreid, J. Phys. (Paris) **39**, 1253 (1978); E. L. Koschmieder and J. R. Campbell, to be published.

[6a]E. Palm, J. Fluid Mech. **8**, 183 (1960).

[6b]L. A. Segel and J. T. Stuart, J. Fluid Mech. **13**, 289 (1962).

[6c]F. H. Busse, J. Fluid Mech. **30**, 625 (1967).

[7a]M. N. Roppo, S. H. Davis, and S. Rosenblatt, Phys. Fluids **27**, 796 (1984).

[7b]P. C. Hohenberg and J. Swift, Phys. Rev. A **35**, 3855 (1987).

[7c]C. W. Meyer, G. Ahlers, and D. Cannell, Phys. Rev. Lett. **59**, 1577 (1987).

[8]S. Ciliberto, F. Francini, and F. Simonelli, Opt. Commun. **54**, 381 (1985).

[9]S. Ciliberto and M. A. Rubio, Phys. Rev. Lett. **58**, 2652 (1987).

[10]G. S. Charlson and R. L. Sani, Int. J. Heat Mass Transfer **13**, 1479 (1970).

[11]The uncertainty on the liquid depth (about 1%) gives an error of 0.1 K in the calculation of this theoretical value.

[12]To obtain this value, the finite thermal conductivity of the sapphire plate has been taken into account. The main source of error in the determination of the threshold is the estimation of the heat losses.

[13]G. Ahlers, D. Cannell, and V. Steinberg, Phys. Rev. Lett. **54**, 1373 (1985); M. S. Heutmaker, P. N. Fraenkel, and J. P. Gollub, Phys. Rev. Lett. **54**, 1369 (1985).

[14]G. Ahlers, M. C. Cross, P. C. Hohenberg, and S. Safran, J. Fluid Mech. **110**, 297 (1981).

[15]M. C. Cross, Phys. Fluids **23**, 1727 (1980).

[16]A. Schlüter, D. Lortz, and F. H. Busse, J. Fluid Mech. **23**, 129 (1965).

[17]R. W. Walden and G. Ahlers, J. Fluid Mech. **109**, 89 (1981).

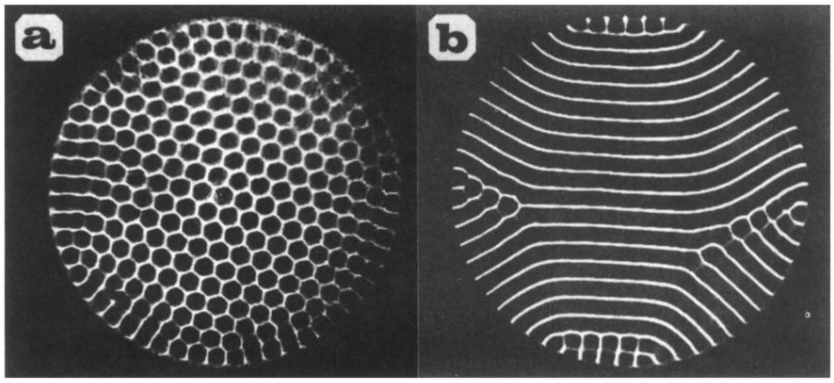

FIG. 1. Shadowgraph images of convective patterns. (a) Hexagonal pattern for $\epsilon = 0.02$. (b) Pattern of rolls for $\epsilon = 0.14$.

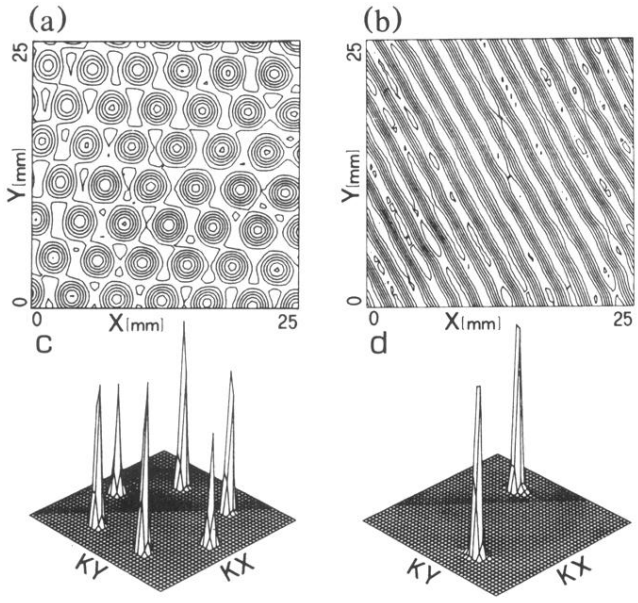

FIG. 2. Temperature-field reconstruction from the horizontal gradient. (a) Hexagonal pattern for $\epsilon = 0.02$. The temperature difference between two isotherms is 0.21 K. (b) Rolls for $\epsilon = 0.14$. The isotherms are separated by 0.42 K in this case. Fourier spectra of the temperature field in the full scanning area for the same values of ϵ as in (a) and (b): (c) for hexagons; (d) for rolls.